



FORMATION ENERGIES OF COMPLEXES OF HYDROGEN AND CARBON ATOMS WITH VACANCY IN FCC ALUMINUM FROM FIRST-PRINCIPLES

Vo Duy Dat, A.G. Lipnitskii, Do Duc Tam

Belgorod State University,
Pobedy St., 85, Belgorod, 308015 Russia

Abstract. The DFT calculations are performed to investigate the interactions of hydrogen and carbon atoms with vacancy in fcc aluminum. The solution energies of hydrogen and carbon atoms in aluminum, the cohesive energies of these atoms with vacancy and the formation energies of impurity-vacancy complexes were calculated. We show that the carbon-hydrogen bonding not only increases the cohesive energy of carbon-vacancy complex but also makes the vacancy formation energy negative by forming carbon-hydrogen-vacancy complex.

Keywords: first-principle calculations, aluminum, carbon-hydrogen bond, impurity-vacancy complexes, formation energy.

1. Introduction. Structural components made from aluminum and its alloys are vital to the aerospace industry and are important in many areas of transportation and structural materials for their low density and ability to resist corrosion due to the phenomenon of passivation. Generally, the mechanical properties of solids are sensitive to presence of impurity light atoms. Small concentrations of impurity atoms in bulk aluminum can drastically change the response of aluminum to external loading [1–3]. Aluminum has been the subject of various experimental and theoretical investigations regarding the effects of hydrogen impurities. Two major effects of hydrogen on the properties of aluminum are hydrogen-enhanced local plasticity [4, 5] and hydrogen embrittlement (HE) [6, 7]. HELP takes places only when the diffusion of H atoms is fast enough to allow them to redistribute around the core of a moving dislocation (dynamic trapping) and thereby continuously minimize the system energy [8]. HE is widely known to be caused by the H-enhanced dislocation mobility [8]. According to the study using of density-functional theory (DFT) of G. Lu and E. Kaxiras [9], another mechanism of HE is the interaction of hydrogen and vacancy. Hydrogen atoms are observed experimentally that during hydrogen charging, they immediately interact with vacancies on the surface of aluminum, forming surface bubbles or resulting in the diffusion of hydrogen-vacancy complexes into the bulk of aluminum [10]. G. Lu and E. Kaxiras suggest that hydrogen lower the vacancy formation energy and through this it affects on the rate of void formation in aluminum. However experimental measurement of Shimomura and Yoshida shows new results which are not completely understood [11]. They use highly pure aluminum for their experiments (very low concentration of hydrogen impurities left in this sample). The results show that without the removal of hydrogen, adding carbon to aluminum causes more void formation than adding hydrogen to this specimen. But the rate of void formation decreases significantly when hydrogen atoms are removed from aluminum before carbon is added to this specimen. From these results, we can see that small concentration of hydrogen may result in large effect on void formation, and besides hydrogen, other light atoms may affect the formation of voids in bulk aluminum. Moreover, for a not highly pure



aluminum with many light impurity atoms, it is not the interaction of vacancy and hydrogen but the interactions of point defects including impurity atoms and vacancy play important roles in the changing of the properties of aluminum. Despite the importance of these interactions, detailed studies about them are still lacking. It is difficult to determine the concentration of H in bulk Al by experimental measurements because its solubility is extremely low and the results are dependent on H charging conditions. In this paper we study the interactions hydrogen, carbon and vacancy point defects, the forming of the complexes from these defects in fcc lattice of aluminum using DFT which was used successfully for studying the interactions of hydrogen with aluminum [9].

2. Calculation method. The DFT calculations are performed with using of a plane-wave basis and the projector-augmented wave (PAW) method [12] as implemented in the ABINIT code. The generalized-gradient approximation [13] is used for the exchange-correlation energy. The plane-wave kinetic-energy cutoff E_{cut} of 800 eV and the k-point meshes for the different $2 \times 2 \times 2$ super-cells of fcc lattice are chosen to guarantee an total energy accuracy of 1 meV/atom. We also investigate the convergence of the formation energies of the complexes of point defects according to E_{cut} in the range of 300-800 eV. Molecular dynamic of Nose-Hoover thermostat [14] based on the Verlet algorithm [15] was used with temperature 300 K and then 100 K to determine the atomic configuration of super-cells with point defects and their complexes at low temperatures. Energetic characteristics of different configurations were calculated after full relaxation of the super-cells using the Broyden-Fletcher-Goldfarb-Shanno [16] minimization in which the interaction forces between atoms should not be greater than 2.5 meV/Å. For visualization of the positions of octahedral, tetrahedral interstitial sites and aluminum vacancy we show part of the super-cell that contains these positions in Fig. 1.

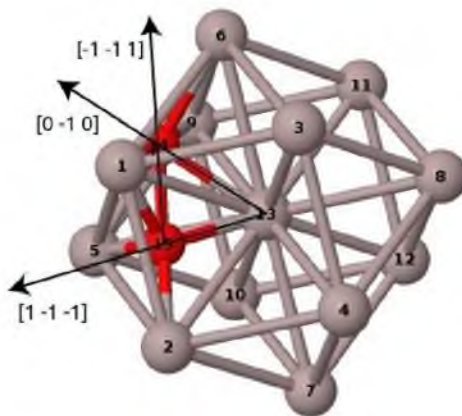


Fig. 1. The part of super-cells including impurity atoms at the octahedral and tetrahedral interstitial sites (the red balls with number 14 and 15 respectively). The aluminum atom with number 13 will be removed when we perform calculations that relate to the aluminum vacancy.

Because of the lack of experimental data about solution energies of carbon in bulk Al we try to make our calculations as reliable as possible by a series of systematical tests before choosing the PAW potentials for aluminum, hydrogen and carbon. The accuracy of PAW potentials is tested by comparing all the experimental measurements that we can find with our calculated results such as the lattice constants of FCC aluminum, the bond-length of H-C molecule, the formation energy of single aluminum vacancy and the solution energy of hydrogen in bulk aluminum. The PAW-potentials are based on by good reproduction of experimental data and good convergence according



to the cutoff energy. Our lattice constant of pure FCC aluminum equals 4.13 Å which is close to the experimental value (4.05 Å) [17]. The results of other testing calculations will be shown below.

3. Results and discussions.

3.1. Solution of hydrogen and carbon in bulk aluminum. The solution energies of a hydrogen atom or a carbon atom in fcc lattice of aluminum are calculated by following formula

$$E_S^X = E[X^{T/O} + Al_{32}] - E[Al_{32}] - 1/2 \cdot E[X_2]. \quad (1)$$

In Eq. 1 E_S^X are the solution energies of atom X (X = hydrogen or carbon) at the interstitial sites in fcc lattice, $E[X^{T/O} + Al_{32}]$ is the total energy of the super-cell with impurity atom X at tetrahedral (T) or octahedral (O) interstitial site, respectively, and $E[Al_{32}]$ is the energy of the super-cell without any impurity atom. $E[X_2]$ is the energy of molecule H_2 in the vacuum in the case $X = H$ or the energy of 2 carbon atoms in diamond lattice in the case $X = C$. In table 1 we show the convergence of solution energies E_S of the impurity atoms according to Ecut which ranges from 300 eV to 800 eV.

Table 1

Calculated solution energy E_S of hydrogen atom (H) and the carbon atom (C) at tetrahedral (tet) and octahedral (oct) interstitial sites.

Configuration	Ecut (eV)					
	300	400	500	600	700	800
	E_S (eV)					
H_tet	0.84	0.76	0.72	0.70	0.69	0.69
H_oct	0.98	0.90	0.86	0.85	0.84	0.83
C_tet	3.19	1.92	1.46	1.31	1.27	1.26
C_oct	3.09	1.85	1.40	1.25	1.21	1.20

As we can see from the results of computational calculations showed in table 1, the difference in solution energies E_S according to Ecut for all impurity atoms is not larger than 0.01 eV between the calculations with Ecut of 800 eV and of 700 eV. So we decide that the ecut of 800 eV gives us convergent values and we refer to all DFT data below as those calculated with the use of ecut 800 eV.

The value of solution energy of hydrogen at tetrahedral site from experiments ranges from 65 to 71 eV [18–21]. DFT calculations of other authors produce hydrogen solution energies from 69 to 71 eV [22] for tetrahedral site and from 0.76 to 0.82 eV [22] for octahedral site. In the case of hydrogen adsorption, our results are very close to experimental and theoretical results of other authors. We do not have published data of the solution energy of carbon in fcc aluminum lattice. From our data we consider that carbon atom's preference position in bulk aluminum is octahedral interstitial site.

Because of the fact that the chosen PAW potentials reproduce some good experimental data which are related to hydrogen and carbon atoms in aluminum FCC lattice, we can say that our solution energies of carbon in aluminum lattice are reliable for, at least, the prediction of carbon's preference interstitial position in bulk aluminum.

According to the solution energies we can say that at 0 K hydrogen atom does not dissolve in bulk aluminum because its solution energy is positive. However, at room temperature it is observed

experimentally that about 1000 at. ppm of H atoms can enter Al [23]. For certainty, we use carbon from diamond lattice to calculate the solution energy so it is obviously that the energies of carbon solution can not be negative. But this does not mean that there are not carbon impurity in bulk aluminum as we can see from the work of Shimomura and Yoshida [11] mentioned above.

3.2. Interaction of Carbon with a vacancy and a vacancy–hydrogen complex in fcc lattice of aluminum. The formation of complexes of point defects really affects their concentration, diffusibility and the behavior in material. For example, the formation of the complex from hydrogen and vacancy may significantly increase the concentration of vacancy in aluminum [11]. In order to study the properties of the complex of point defects it is necessary to determine the atomic structure of this complex corresponding to minimum energy. This can be done by the relaxation procedure of some beginning configuration of complex to the equilibrium configuration.

In the case of interstitial impurity solution we know that center of the interstitial site corresponds to reasonable beginning position of the impurity for relaxation the system to equilibrium configuration. In the case of vacancy, although the space around the aluminum vacancy is symmetric, it does not mean that the configuration with impurity atom at the center of the vacancy is the equilibrium one, especially when there are two atoms inside the vacancy. Moreover, if the beginning positions of atoms are close to some local minimum energy, the optimization process may give us a metastable configuration. So we need one more step before the optimization to determine the beginning positions of atoms inside vacancy so that optimization process can give us the equilibrium configuration. It is the Nose–Hoover thermostat [14] with Verlet algorithm [15], the temperature is set to 300K to give the atom enough energy so that it can move out of or across local minimums, then the movement of atom is slowed down by setting temperature to 100K. This process makes it possible for the atom to go to the position where the total energy of the system is the closest to the global minimum. This process followed by the relaxation with the Broyden–Fletcher–Goldfarb–Shanno minimization [16]. Fig. 2 shows the configurations of a carbon-vacancy complex C-V and a hydrogen-vacancy complex H-V, which are received by performing the method mentioned above.

The atomic configuration of carbon-hydrogen-vacancy complex (C-H-V) is received by the same method above including the use of molecular dynamical and systematical relaxation. In this case, the carbon atom is initially embedded into the center of the vacancy of relaxed H-V complex. The configuration after relaxation is shown in Fig. 2b. Fig. 3 shows the atomic configuration of C-H-V complex after performing the molecular dynamics simulation followed by the relaxation process. After the optimization, carbon and hydrogen exchange the position with each other. They create C-H bond in which hydrogen atom turns toward the center of the vacancy and carbon atom associates with three nearest neighbored aluminum atoms.

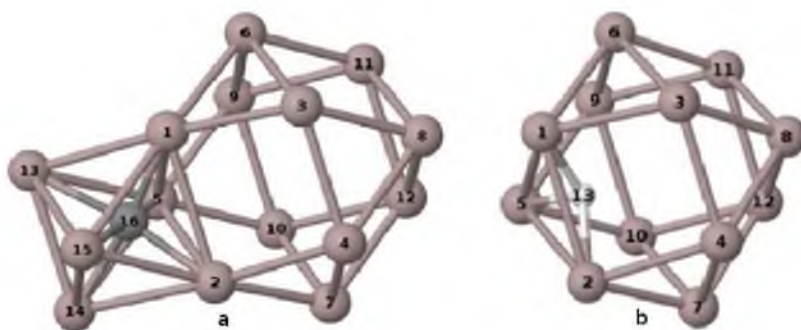


Fig. 2. The parts of super-cells including the relaxed complexes of impurity atoms and the

vacancy in fcc lattice of Al. a – the complex of carbon atom (grey ball with number 16) and single vacancy, b – the complex of hydrogen atom (white ball with number 13) and single vacancy.

Thermodynamical profit of developing the number of point defects in a complex is determined by the cohesive energy of new defect to the complex with smaller size. In our considered complexes, the cohesive energies are calculated by the following formulas

$$E_C^{X-V} = E[X^{T/O} + Al_{32}] + E[V + Al_{31}] - E[Al_{32}] - E[X - V + Al_{31}], \quad (2)$$

$$E_C^{C-(H-V)} = E[C^O + Al_{32}] + E[H - V + Al_{31}] - E[Al_{32}] - E[C - H - V + Al_{31}], \quad (3)$$

$$E_C^{H-(C-V)} = E[H^T + Al_{32}] + E[C - V + Al_{31}] - E[Al_{32}] - E[C - H - V + Al_{31}]. \quad (4)$$

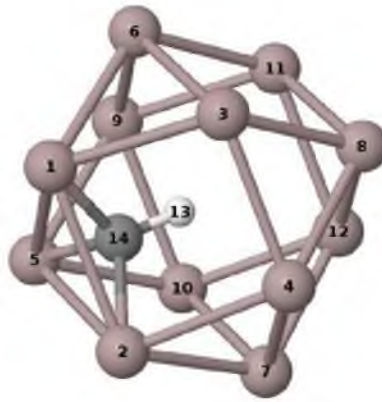


Fig. 3. The part of super-cells including the carbon-hydrogen-vacancy complex (C-H-V). Grey ball number 14 is carbon atom and small white ball number 13 is hydrogen atom.

In Eq. 2, 3 and 4 E_C^{X-V} is the cohesive energy of X atom (X= hydrogen or carbon) with vacancy V, $E_C^{C-(H-V)}$ is the cohesive energy of C with H-V complex, $E_C^{H-(C-V)}$ is the cohesive energy of H with C-V complex, $E[Al_{32}]$ is total energy of the super-cell with 32 aluminum atoms, $E[X_{T/O} + Al_{32}]$ is total energy of the super-cell with 32 aluminum atoms and an impurity atom at tetrahedral T (X=H) or at octahedral O (X=C) interstitial sites, $E[V + Al_{31}]$ is total energy of the super-cell with 31 aluminum atoms and a vacancy, $E[X^{\circ}V + Al_{31}]$ is total energy of the super-cell with atom X connected to the vacancy, $E[C^{\circ}H^{\circ}V + Al_{31}]$ is total energy of the super-cell with the molecule C-H inside the vacancy. The table 2 lists the calculated cohesive energies.

Table 2

Cohesive energies E_C^{H-V} , E_C^{C-V} , $E_C^{C-(H-V)}$ and $E_C^{H-(C-V)}$ of H, C atoms to aluminum vacancy, of carbon atom to H-V complex and of hydrogen atom to C-V complex respectively.

E_C (eV)			
E_C^{H-V}	E_C^{C-V}	$E_C^{C-(H-V)}$	$E_C^{H-(C-V)}$
0.39	0.18	0.77	0.98



Our calculated cohesive energy of hydrogen atom to the vacancy is a little larger than the theoretical value 0.33 eV [22] but smaller than the experimental values which ranges from 0.43 to 0.53 eV [24–26]. The cohesive energy of carbon atom with the vacancy is 0.18 eV less than the one of hydrogen with vacancy (0.39 eV), but it is high enough to make sure that C-V complex is stable one at moderate temperature. Moreover adding a carbon atom to the H-V complex or adding a hydrogen atom to the C-V complex increases the cohesive energy of these complexes by the same value 0.59 eV. We can say that both carbon and hydrogen from interstitial sites are easily trapped by the impurity-vacancy complex to form the C-H bond inside the vacancy. Similar formation of C-H bond inside vacancy of tungsten was obtained by S. Jin and other co-workers from pseudopotential plane-wave method [27]. However, the formation effect of such bond in tungsten is weaker than in aluminum and carbon causes a small decreasing of cohesive energy of hydrogen with vacancy, the difference is only -0.03 eV. To understand more about how the bond creating between H and C atoms changes their interaction with the vacancy we investigate the distribution of density of valence electrons near C-H bond. Fig. 4 shows our calculated distribution of density.

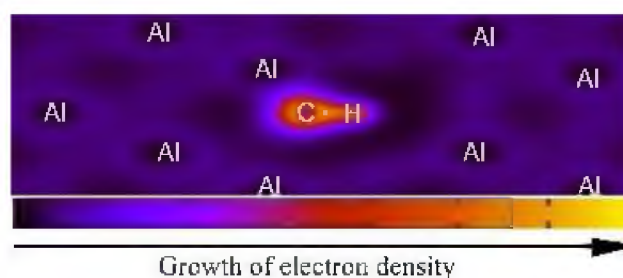


Fig. 4. The distribution of electron density around C-V-H complex. The plane of this picture goes through the positions of carbon atom, hydrogen atom and aluminum atom (atoms with number 14, 13 and 5, respectively in Fig. 3).

In Fig. 4, it can be seen enlarging of the valence density on the line between carbon and hydrogen atoms. This shows the covalent character of C-H bond in the aluminum vacancy and causes an interest of comparing this bond with the one in free CH_4 molecule. The length of a so-formed C-H bond is 1.11 Å, similar to the C-H bond length in a CH_4 molecule (1.084 Å) [28].

3.3. Effects of impurities on formation energy of vacancy. At fixed thermodynamic condition the concentration of vacancy in metal should be constant. However vacancy concentration may be changed by the interaction with impurity atoms in which different impurity-vacancy complexes are formed. In the case of aluminum, this phenomenon is experimentally observed by small angle neutron scattering measurements [10]. In our study, we see that not only hydrogen but also carbon can be trapped by vacancy turning vacancies into some complexes. The interaction of carbon impurity with vacancy in aluminum is considered but its mechanism is still unclear from the experimental results of Shimomura and his co-workers [11]. To keep the free vacancy concentration constant other vacancies must be created. Probability of vacancy generation depends on its formation energies. The vacancy formation energies in pure aluminum and in the presence of impurity atoms inside aluminum lattice are calculated by following formulas:



$$E_v^f = E[V + Al_{31}] - 31/32 \cdot E[Al_{32}], \quad (5)$$

$$E_v^f[C] = E_C^{C-V} - E_v^f, \quad (6)$$

$$E_v^f[H] = E_C^{H-V} - E_v^f, \quad (7)$$

$$E_v^f[C + H] = E_v^f[H] - E_C^{C-(H-V)}. \quad (8)$$

In Eq. 5, 6, 7 and 8 E_v^f , $E_v^f[C]$, $E_v^f[H]$, and $E_v^f[C + H]$ are the vacancy formation energies in pure aluminum, in the presence of carbon atom at the octahedral interstitial site of fcc aluminum lattice, in the presence of hydrogen atom at the tetrahedral interstitial site of fcc aluminum lattice, in the presence of both carbon and hydrogen atoms at the interstitial site of fcc aluminum lattice, respectively. Other values in formulas from (5) to (8) were mentioned in previous paragraphs. Table 3 lists our calculated formation energies of the vacancies.

Table 3

Formation energies of vacancies in pure aluminum – E_v^f , in aluminum with C impurity – $E_v^f[C]$, with H impurity – $E_v^f[H]$ and with both H and C impurity atoms – $E_v^f[H + C]$.

E_v (eV)			
E_v^f	$E_v^f[C]$	$E_v^f[H]$	$E_v^f[H + C]$
0.55	0.37	0.16	-0.61

Our vacancy formation energy in bulk aluminum is about 2% different from those received by ab initio calculations of other authors (0.54-0.55 eV) [22, 29, 30] but it is 18% different from the experimental values (0.63-0.67 eV) [31, 32]. However, the experiments are typically performed at high temperatures to have a measurable concentration of vacancies, while the our DFT calculations correspond to 0 K. Empirical potential molecular dynamics simulations [33] indicate that the vacancy formation enthalpy decreases by about 0.08 eV as the temperature decreases from the melting point of 933 to 0 K. Thus, the "measured" vacancy formation enthalpy at 0 K may be estimated roughly as 0.63 eV. Based on this estimation, the uncertainty of our vacancy formation energy is not more than 6%.

As we can see from table 3 that the vacancy formation energy decreases from 0.55 eV with pure aluminum to 0.37 eV when the vacancy forms the complex with a carbon atom in aluminum. The same formation energy decreases to 0.16 eV when the H-V complex is formed. This means that it is easier to form vacancies when there is carbon or hydrogen impurity in the aluminum lattice. But the formation of vacant node in fcc lattice of aluminum releases energy 0.61 eV when the C-H-V complex is formed. This explains a significant increasing of void concentration in bulk aluminum with the presence of both hydrogen and carbon defects, which is experimentally observed by Y. Shimomura and his co-workers [11].

4. Conclusion. Using density functional theory calculations, we investigated the interactions of impurity atoms and vacancy and the formation of stable complexes of these point defects in fcc lattice of aluminum. The results of this work can be summarized as follows:

- Both hydrogen and carbon atoms can be trapped by vacancy in aluminum. The large cohesive energy of a hydrogen atom with vacancy leads to the high rate of the hydrogen-vacancy complex formation, this supports the experimental fact that during hydrogen charging, very little amount



of hydrogen diffuses into the bulk of aluminum [10]. Hydrogen atoms interact with vacancies on the surface of aluminum creating hydrogen-vacancy complexes which then diffuse into bulk of aluminum [10].

- From the decreasing of vacancy formation energies by the presence of impurity atoms we suggest that the rate of void formation in bulk aluminum will increase. Our assumption is in good agreement with the experimental results of Y. Shimomura and his co-workers [11] which show that the presence of both hydrogen and carbon atoms in bulk aluminum make the void concentration be the largest in comparison with the cases when only carbon atom or hydrogen atom are introduced to bulk aluminum.

- We found the formation of C-H bond inside aluminum vacancy, which plays an important role in the interaction of vacancy with impurity atoms. Adding a second impurity to the impurity-vacancy complex makes the cohesive energy increase by 0.55 eV and the formation energy of vacant nodes in fcc aluminum changes from positive into negative value owing to formation of hydrogen-carbon-vacancy complex.

Investigating carbon, hydrogen and vacancy point defects in bulk aluminum, we see that not only the behaviors of each of them affects on the properties of aluminum but the interactions between them also play important role in the changing of aluminum's properties. The hydrogen embrittlement process in aluminum may be significantly affected by the third point defect — carbon atom, besides the vacancy and hydrogen. Because of the important effects of point defects on the properties of aluminum, more studies about them need to be carried out to improve the performance of aluminum and its alloys in different environments.

References

1. Zamora R.J., Nair A.K., Hennig R.G., Warner D.H. Ab initio prediction of environmental embrittlement at a crack tip in aluminum // *Physical Review B*. – 2012. – 86. – P.060101(R).
2. Aoki Y., Fujii H., Nogi K. Effect of atomic oxygen exposure on bubble formation in aluminum alloy // *Journal of Materials Science*. – 2004. – 39. – P.1779–1783.
3. Turner D.E., Zhu Z.Z., Chan C.T., Ho K.M. Energetics of vacancy and substitutional impurities in aluminum bulk and clusters // *Physical Review B*. – 1997. – 55. – P.13842–13852.
4. Bond G.M., Bond G.M., Robertson I.M., Birnbaum H.K. Effects of hydrogen on deformation and fracture processes in high-purity aluminium // *Acta Metallurgica*. – 1988. – 36;№8. – P.2193–2197.
5. Lu G., Zhang Q., Kioussis N., Kaxiras E. Hydrogen-Enhanced Local Plasticity in Aluminum: An Ab Initio Study // *Physical Review Letters*. – 2001. – 87. – P.095501.
6. Watakabe T., Itoh G., Hatano Y. Visualization of Diffusive Hydrogen // *Materials Science Forum*. – 2010. – Vols. 654–656. – P.2903–2906.
7. Kumar, S. Precipitation hardening and hydrogen embrittlement of aluminum alloy AA7020/ S. Kumar and T K G Namboodhiri.// *Bulletin of Material Science*– 2011.–Vol. 34.–№. 2.–P. 311–321
8. Myers S.M., Baskes M.I., Birnbaum H.K., Corbett J.W., DeLeo G.G., Estreicher S.K., Haller E.E., Jena P., Johnson N.M., Kirchheim R., Pearton S.J., Stavola M.J. Hydrogen interactions with defects in crystalline solids // *Reviews of Modern Physics*. – 1992. – 64. – P.559.
9. Lu G., Kaxiras E. Hydrogen Embrittlement of Aluminum: The Crucial Role of Vacancies // *Physical Review Letters*. – 2005. – 94. – P.155501.
10. Rozenaka P., Siroisa E., Ladnaa B., Birnbaum H.K., Spooner S. Characterization of hydrogen defects forming during chemical charging in the aluminum // *Journal of Alloys and Compounds*. – 2005. – 387. – P.201–210.
11. Shimomura Y., Mukouda I., Chen Q.R., Diaz de la Rubia T. Impurity Atoms Responsible for the Void Formation in Quenched Pure Aluminum // *Materials Transactions*. – 1995. – 36;№3. – P.413–419.



12. Blöchl P.E. Projector augmented-wave method // *Physical Review B*. – 1994. – 50. – P.17953–17979.
13. Perdew J.P., Chevary J.A., Vosko S.H., Jackson K.A., Pederson M.R., Singh D.J., Fiolhais C. Atoms, molecules, solids, and surfaces: Applications of the generalized gradient approximation for exchange and correlation // *Physical Review B*. – 1992. – 46. – P.6671–6687.
14. Evans D.J., Holian B.L. The Nose–Hoover thermostat // *Journal of Chemical Physics*. – 1985. – 83. – №8. – P.4069.
15. Verlet L. Computer 'experiments' on classical fluids. I. Thermodynamical properties of Lennard-Jones molecules // *Physical Review* – 1967. – Vol. 159. – P. 98–103
16. Head J.D., Zerner M.C. A Broyden–Fletcher–Goldfarb–Shanno optimization procedure for molecular geometries // *Chemical Physics Letters*. – 1985. – 122; №3. – P.264–270.
17. Jacobs P.W.M., Zhukovskii Yu.F., Mastrikov Yu., Shunin Yu.N. Bulk and Surface Properties of Metallic Aluminium: DFT Simulations, Computer Modelling and New Technologies // *Computer Modelling and New Technologies*. – 2002. – 6; №1. – P.7–28.
18. Edwards R.A.H., Eichenauer W. Reversible hydrogen trapping at grain boundaries in super-pure aluminium // *Scripta Metallurgica*. – 1981. – 14. – P.971.
19. Eichenauer W., Hattenbach K., Pebler A. The solubility of hydrogen in solid and liquid aluminum // *Zeitschrift Fur Metallkunde*. – 1961. – 52. – P.682.
20. Sugimoto H., Fukai Y. Solubility of hydrogen in metals under high hydrogen pressures: thermodynamical calculations // *Acta Metallurgica et Materialia*. – 1992. – 40. – P.2327–2336.
21. Ichimura M., Katsuta H., Sasajima Y., Imabayashi M. Hydrogen and deuterium solubility in aluminum with voids // *Journal of Physics and Chemistry of Solids*. – 1988. – 49. – P.1259.
22. Wolverton C., Wolverton C., Ozolins V., Asta M. Hydrogen in aluminum: First-principles calculations of structure and thermodynamics // *Physical Review B*. – 2004. – 69. – P.144109.
23. Buckley C.E., Birnbaum H.K., Bellmann D., Staron P. Calculation of the radial distribution function of bubbles in the aluminum hydrogen system // *Journal of Alloys and Compounds*. – 1999. – Vols.293–295. – P.231–236.
24. Linderöth S. Hydrogen diffusivity in aluminium // *Philosophical Magazine Letters*. – 1988. – 57. – P.229.
25. Linderöth S., Rajainmaki H., Nieminen R.M. Defect recovery in aluminum irradiated with protons at 20 K // *Physical Review B*. – 1987. – 35. – P.5524.
26. Myers S.M., Besenbacher F., Norskov J.K. Immobilization mechanisms for ion?implanted deuterium in aluminum // *Journal of Applied Physics*. – 1985. – 58. – P.1841.
27. Jin S., Liu Y.L., Zhou H.B., Zhang Y., Lu G.H. First-principles investigation on the effect of carbon on hydrogen trapping in tungsten // *Journal of Nuclear Materials*. – 2011. – 415; №1. – P.S709–S712.
28. Melissas V.S., Truhlar D.G. Deuterium and carbon?13 kinetic isotope effects for the reaction of OH with CH₄ // *Journal of Chemical Physics*. – 1993. – 99. – P.3542.
29. Mattsson T.R., Mattsson A.E., Sandberg N., Grimvall G. Vacancies in Metals: From First-Principles Calculations to Experimental Data // *Physical Review Letters*. – 2000. – 85. – P.18.
30. Vita A.D., Gillan M.J. The ab initio calculation of defect energetics in aluminium // *Journal of Physics: Condensed Matter*. – 1991. – 3; №33. – P.6225–6237.
31. Hehenkamp T. Absolute vacancy concentrations in noble metals and some of their alloys // *Journal of Physics and Chemistry of Solids*. – 1994. – 55. – P.907.
32. Lynn K.G., Schultz P.J. Vacancy formation energy measurements in single crystal aluminum using a variable-energy positron beam // *Applied Physics A*. – 1985. – 37; №1. – P.31–36.
33. Fluss M.J., Smedskjaer L.C., Chason M.K., Legnini D.G., Siegel R.W. Measurements of the vacancy formation enthalpy in aluminum using positron annihilation spectroscopy // *Physical Review B*. – 1978. – 17. – P.3444.